
Adsorption-desorption kinetics of phosphate between sediment and water in coastal areas

Andrieux-Loyer Françoise ^{1,*}, Aminot Alain ¹

¹ Ifremer, DYNECO, F-29280 Plouzané, France

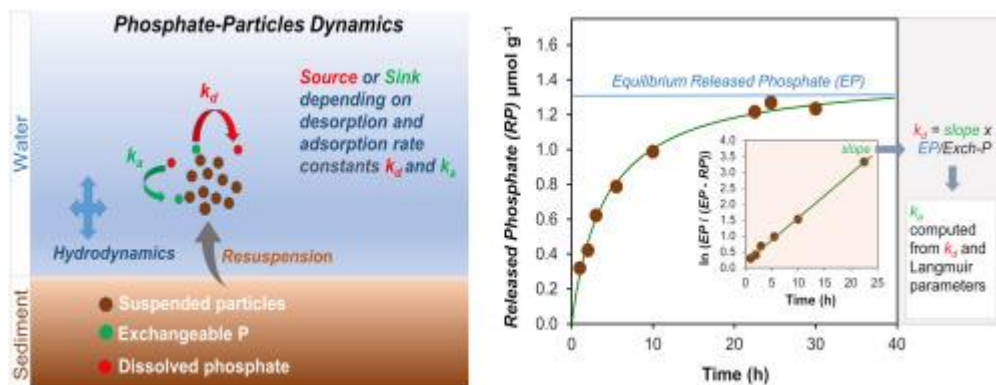
* Corresponding author : Françoise Andrieux-Loyer, email address : Francoise.Andrieux@ifremer.fr

Abstract :

In this article the kinetics of adsorption-desorption processes of phosphate on sediments is studied according to the Langmuir theory. The theoretical developments are described and applied to the laboratory experiments which rely on desorption of adsorbed phosphate from coastal and estuarine sediments.

Desorption (k_d) and adsorption (k_a and $k_a Q^\circ$) rate constants were determined using sediments from various areas with a wide range of grain size characteristics. Accurate determination of k_d is of primary importance since desorption may directly enhance algal growth. At a temperature of 20 °C, values of k_d range from 0.057 h⁻¹ to 0.128 h⁻¹. The results show that the use of k_a , deduced from the Langmuir coefficient b ($b = k_a/k_d$), is not recommended since this coefficient is affected by poor precision. Alternatively, adsorption rates can use the more reliable combined constant $k_a Q^\circ$. Values of $k_a Q^\circ$ range from 0.013 to 0.054 L g⁻¹ h⁻¹ (20 °C). The sediment grain size has only moderate influence on the rate constants. The relationship of these rate constants with temperature was studied in the range 1–30 °C, encountered in most marine areas. The exponential law with temperature is determined and an increase factor of 1.6 is found for each 10 °C increase. This work has strong implications for environmental modelling to encompass the sediment phase as a contributor to the cycling of essential nutrients in estuarine and coastal systems.

Graphical abstract



Highlights

► Kinetics of Langmuir-treated phosphate exchange between coastal sediments and water. ► Determination of rate constants with highlight on a combined adsorption constant. ► Adsorption and desorption rate constants: little dependent on sediment grain size. ► The temperature factor of rate constants is 1.6 for each 10 °C in the range 1–30 °C.

Keywords : exchangeable phosphate, sediment, adsorption, desorption, kinetics

64 1. INTRODUCTION

65 Eutrophication induced by nitrogen and phosphate enrichment in estuarine and coastal areas has been well
66 documented (Boesch, 2002; Seitzinger et al., 2005). Because of the various interactions of phosphate with the solid
67 phase, sediment is a potential phosphate reservoir which may enrich the water column when there is a high demand
68 during intense primary producer growth (Van Raaphorst et al., 1994; Smil, 2000). In oxic coastal and estuarine
69 areas, phosphate concentration is mostly governed by adsorption-desorption of exchangeable phosphate while
70 precipitation and oxidation-reduction of phosphate compounds are mechanisms of minor importance. This most
71 labile phosphate form at the solid-water interface may significantly contribute to the final trophic level of water
72 bodies (Jarvies et al., 2002; Zhang et al., 2012) and induce possible growth of toxic algae.

73 Models of sediment diagenesis have become essential tools for environmental management by integrating
74 physical, bacteriological and planktonic processes, however adsorbed phosphate generally plays a minor role in
75 these models since it is often included in the iron-bound P fraction (Cha et al., 2005; Ait Ballagh et al., 2020,
76 2021). In contrast, in coastal waters where eutrophication events are expected, the contribution of exchangeable
77 phosphate is of primary importance as opposed to forms strongly bound to the sediment. Couceiro et al. (2013)
78 showed that by omitting resuspension in a North Sea biochemical model (Baretta et al., 1995) the use of diffusive
79 fluxes of interstitial nutrient concentrations, led to a large underestimation of nutrients concentrations in the water
80 column, and more particularly those of phosphate (from the adsorbed fraction (Sondergaard et al., 1992)).
81 However, sediment-water phosphate exchanges due to the adsorption-desorption process have, until now, been
82 poorly treated because of the unavailability of reliable constants. Up to now, research about phosphate sorption
83 processes has mainly focused on adsorption (Zhou et al., 2005; Wang et al., 2012; Li et al., 2013; Otero et al.,
84 2013; Wang et al., 2022), with little attention towards desorption with the exception of the study of Wang et al
85 (2022). Among these, adsorption constants can generally be found but rarely desorption constants, despite the
86 importance of the sediment phosphate reservoir which may supply the water column.

87 In a previous article we discussed the determination of the parameters associated with adsorbed phosphate
88 such as the exchangeable phosphate, the partition coefficient and the maximal sediment adsorption capacity using
89 Langmuir's theory as a tool to access this data (Andrieux-Loyer and Aminot, 2023). As the bioavailability of P for
90 phytoplankton depends not only on the quantity of P adsorbed on the sediment but also on the rate of P release, its
91 determination is essential. In this paper the principles of determination of adsorbed phosphate kinetic exchange
92 constants are presented using the Langmuir theory, then applied to the experimental method which are described
93 to obtain these constants. The present work focuses on both desorption and adsorption kinetics processes from

94 experiments based on phosphate exchange from sediments. First, kinetic constants were established at a
 95 temperature of 20 °C, and secondly the temperature dependence of the constants was studied within the range of
 96 1-30 °C most likely encountered in the areas of interest.

97

98 2. THEORETICAL CONSIDERATIONS

99 2.1. Principles of adsorption/desorption processes

100 The adsorbed phosphate exchange process between sediment and water was previously studied to obtain
 101 exchangeable phosphate concentration, partition coefficient and maximal sediment adsorption capacity (Andrieux-
 102 Loyer and Aminot, 2023). The Langmuir theory extended from gas to solid-solution interactions by Voice and
 103 Weber (1983) was used as a tool to provide these parameters. For kinetics considerations, the solid-water exchange
 104 is characterized by adsorption and desorption rates which are treated as first order processes for each reaction
 105 component (Voice and Weber, 1983). The Langmuir monolayer adsorption principle is assumed to remain valid
 106 given the very low phosphate concentrations in coastal and estuarine waters.

107 By convention, desorption is treated as a positive rate for the water body, and adsorption as a negative rate.
 108 In a given water mass, the phosphate concentration of the solid phase is the product of phosphate on the solid
 109 ($\mu\text{mol g}^{-1}$) and solid in the water (g L^{-1}). So, with the rate constants for desorption and adsorption respectively k_d
 110 and k_a :

$$111 \quad \text{Desorption rate: } V_d = \{d([PO_4]_{water})/dt\}_d = k_d[PO_4]_{solid}[solid]_{water} \quad (1)$$

$$112 \quad \text{Adsorption rate: } V_a = -\{d([PO_4]_{water})/dt\}_a = k_a[PO_4]_{water}[free\ sites]_{solid}[solid]_{water} \quad (2)$$

113

114 For consistency with previous papers (Aminot and Andrieux, 1996; Andrieux-Loyer and Aminot, 2023),
 115 the Langmuir nomenclature was used (Table 1). Phosphate concentrations are symbolised in the water by C
 116 ($\mu\text{mol L}^{-1}$) and on the solid by q ($\mu\text{mol g}^{-1}$).

117

118

119

120

121

122

123

124

125 **Table 1 Nomenclature used herein.**

Variable	symbol	unit
Desorption rate	V_d	$\mu\text{mol L}^{-1} \text{h}^{-1}$
Adsorption rate	V_a	$\mu\text{mol L}^{-1} \text{h}^{-1}$
Desorption constant	k_d	h^{-1}
Adsorption constant	k_a	$\text{L } \mu\text{mol}^{-1} \text{h}^{-1}$
Partition coefficient	$K_p = q_e/C_e$	L g^{-1}
Maximal adsorption capacity	Q^o	$\mu\text{mol g}^{-1}$
Langmuir coefficient	$b = k_a/k_d$	$\text{L } \mu\text{mol}^{-1}$
IN BATCH		
Solution volume	V	L
Solid mass	m	g
Solid concentration	$S = m/V$	g L^{-1}
Initial PO_4 conc. in liquid phase	C_i	$\mu\text{mol L}^{-1}$
Initial PO_4 conc. on solid (= exchangeable phosphate 'exch-P')	q_i	$\mu\text{mol g}^{-1}$
PO_4 conc. in liquid phase at time 't'	C_t	$\mu\text{mol L}^{-1}$
PO_4 conc. on solid at time 't'	q_t	$\mu\text{mol g}^{-1}$
PO_4 conc. released from solid at time 't'	$q_{Rt} (= q_i - q_t)$	$\mu\text{mol g}^{-1}$
PO_4 conc. in liquid phase at equilibrium	C_e	$\mu\text{mol L}^{-1}$
PO_4 conc. on solid at equilibrium	q_e	$\mu\text{mol g}^{-1}$
PO_4 conc. released from solid at equilibrium	$q_{Re} (= q_i - q_e)$	$\mu\text{mol g}^{-1}$

126

127 According to the nomenclature, the rates (1) and (2) become:

128
$$V_d = \{dC_t/dt\}_d = k_d q_t S \quad (3)$$

129
$$V_a = -\{dC_t/dt\}_a = -k_a C_t (Q^o - q_t) S \quad (4)$$

130 Solid and water concentrations are stable when the equilibrium is reached ($V_d = V_a$, absolute value), hence:

131

132
$$k_d q_e S = k_a C_e (Q^o - q_e) S \quad (5)$$

133

134 Assuming that Q^o exceeds the equilibrium concentration ($Q^o \gg q_e$), it follows that:

135
$$V_a \approx k_a C_e Q^o S \quad (6)$$

136 and that the partition coefficient at equilibrium is:

137
$$K_p = q_e/C_e = b(Q^o - q_e) \approx bQ^o \quad (7)$$

138

139 The overall treatment of the kinetics data requires first determination of both the exchangeable phosphate
140 (exch-P, symbolised as q_i) and the partition coefficient (K_p), and potentially Q^o and b , obtained by the Infinite
141 Dilution Extrapolation (IDE) experiment (Andrieux-Loyer and Aminot, 2023). The rate constants for desorption
142 (k_d) and adsorption (k_a) are obtained by the kinetics batch experiments.

143

144 2.2. Application to kinetics batch experiments

145 Batch experiments were performed by adding known masses of sediment to fixed volumes of water of
 146 known phosphate concentration. At regular time intervals the concentrations of phosphate in the liquid phase were
 147 measured. In this study, focused on phosphate adsorbed on coastal sediments, natural seawater devoid of phosphate
 148 (Phosphate-Free Seawater (PFS)) was used for all desorption experiments in order to simplify the computations
 149 (Andrieux-Loyer and Aminot, 2023). The low sediment concentrations used in our experiments did not alter the
 150 natural seawater pH.

151 The total exchange rate (equation (3) + (4)) is:

$$152 V_T = k_a C_t (Q^o - q_t) - k_d q_t = k_a q_{Re} (m/V) (Q^o - q_i + q_{Rt}) - k_d (q_i - q_{Rt}) \quad (8)$$

153 Given that V_a and V_d are equal at equilibrium, k_a is expressed as a function of k_d , as follows,

$$154 k_a q_{Re} (m/V) Q^o = k_d (q_i - q_{Re}) \quad (9)$$

$$155 k_a = k_d (q_i - q_{Re}) V / q_{Re} m Q^o \quad (10)$$

156 then k_a is replaced by its value (equation (10)), it comes:

$$157 V_T = k_d (q_i - q_{Rt}) - k_d (q_i - q_{Re}) (q_{Rt} / q_{Re}) (Q^o - q_i + q_{Rt}) / Q^o \quad (11)$$

158 With the hypothesis that $Q^o \gg (q_i + q_{Rt})$: *i.e.* $(Q^o - q_i + q_{Rt}) / Q^o \approx 1$, equation (11) becomes:

$$159 V_T = k_d (q_i - q_{Rt}) - k_d (q_i - q_{Re}) q_{Rt} / q_{Re} \quad (12)$$

160 Or
$$V_T = dq_{Rt} / dt = k_d q_i (q_{Re} - q_{Rt}) / q_{re} \quad (13)$$

161 Thus
$$[q_{Re} / (q_{Re} - q_{Rt})] dq_{Rt} = (k_d q_i) dt \quad (14)$$

162 Integration of equation (14) gives:
$$\ln(q_{Re} / (q_{Re} - q_{Rt})) = (k_d q_i / q_{Re}) t \quad (15)$$

163

164 The equation (15) may also be written using the the measured equilibrium concentration C_e in the solution:

165
$$\ln(C_e / (C_e - C_t)) = (k_d q_i S / C_e) t \quad (16)$$

166

167 **Determination of the desorption rate constant (k_d).** Using equation (15) the function

168 $\ln(q_{Re} / (q_{Re} - q_{Rt}))$ is plotted versus time t . The desorption rate k_d is calculated from the slope according to

169 $k_d = slope \times (q_{Re}/q_i)$, where q_{Re} is the released phosphate at equilibrium for the kinetics experiment and q_i
 170 should have previously been determined by the IDE experiment (Andrieux-Loyer and Aminot, 2023).

171

172 **Determination of the adsorption rate constants (k_a and $k_a Q^\circ$).** Ideally the Langmuir coefficient $b =$
 173 k_a/k_d (Table 1) could be obtained from the IDE experiments together with the determination of Q° (equation
 174 (18) in Andrieux-Loyer and Aminot, 2023). Then, from the Langmuir coefficient b , the adsorption rate constant
 175 k_a is calculated as $k_a = bk_d$. Because b and Q° can not be obtained with a good precision, as previously
 176 mentioned (Andrieux-Loyer and Aminot, 2023), we recommend to use the combined constant $k_a Q^\circ$ which can
 177 be obtained considering the partition coefficient $K_p = bQ^\circ$ (equation (7)). Thus, using $b = k_a/k_d$, $K_p =$
 178 $k_a Q^\circ/k_d$ and it comes $k_a Q^\circ = k_d K_p$.

179 3. MATERIAL AND METHODS”

180 3.1. Sampling and storage

181 Sediments were sampled in four main French coastal and estuarine areas, with varying types of sediments,
 182 over the 1991 – 2005 period (details in Andrieux-Loyer and Aminot, 2023). In addition, four samples were selected
 183 from small western France estuaries to enlarge the range of grain size characteristics. The superficial 2 cm layer
 184 of the sediments was collected using a Shipek grab. Almost every experiment was carried out immediately on
 185 board. When this was not possible, the samples were immediately frozen (-20 °C) in polycarbonate vials for further
 186 freeze-drying at the shore laboratory, then sieved at 500 μm before use (Andrieux-Loyer and Aminot, 2023).
 187 Similar results were obtained with fresh and lyophilized sediments as shown Fig. 1.

188 3.2. Laboratory experimental procedures

189 3.2.1. Analytical conditions

190 The concentration of phosphate was determined using Segmented Flow Analysis (SFA; Aminot et al., 2009)
 191 with conditions close to those of Murphy and Riley (1962). Precision within series is about 0.005 $\mu\text{mol L}^{-1}$.

192 Phosphate-Free Seawater (PFS; salinity: 35 ± 0.2) was obtained from coastal seawater collected in late
 193 spring, filtered at about 20-50 μm and stored in a non-opaque carboy at ambient light and temperature in the
 194 laboratory for a minimum of two months (Aminot et al., 2009). Phosphate, removed by the remaining

195 phytoplankton stays close to the detection level. The water is filtered just before use through Whatman GF/F glass
196 fiber filters (~ 0.7 μm pore size).

197 **3.2.2. Kinetics experiments**

198 A series of fixed amounts of solid were added to 7-12 flasks containing natural PFS poisoned with mercuric
199 chloride (40 mg L^{-1}) to prevent any biological interference. The sediments amounts were measured using a small
200 calibrated spoon for wet sediments (on-board experiments) and weighted for lyophilized sediments. Solid to liquid
201 ratio between 0.2 and 0.6 g L^{-1} were used (constant for each batch). Experiments were performed at 20 °C and the
202 flasks were placed on a shaking table. At predetermined time intervals (up to 50 h), the medium was homogenized
203 then an aliquot was centrifuged (3000 $\times g$, 10 min) and the supernatant was collected and frozen for subsequent
204 phosphate determination. For fresh experiments, sediment remaining after collection of the supernatant was kept
205 for mass determination at the laboratory.

206 From the experimental data, calculation of the rate constant k_d requires the determination of the released
207 phosphate concentration after equilibrium is reached, q_{Re} . According to Voice and Weber (1983), the solid water
208 exchanges are treated as first order processes and therefore, q_{Re} , was computed by a first-order kinetic equation of
209 the TableCurve software (#8143, termed 'Equilibrium concentration').

210 In addition, a study of temperature effect on rate constants was carried out using a sediment from the Bay
211 of Seine (French coast of English Channel), with an exchangeable phosphate concentration of 2.46 $\mu\text{mol g}^{-1}$ (pre-
212 determined using the IDE method). A series of kinetics at 1, 10, 20 and 30 °C was performed by placing the
213 experimental flasks in incubators. Flasks containing PFS were pre-conditioned at the corresponding temperature
214 before addition of the sediment. The samples were manually shaken from time to time and their treatments were
215 similar to those described above for experiments at 20 °C. The duration of experiment was increased to 200 and
216 400 h for 10 °C and 1 °C, respectively.

217 **4. RESULTS**

218 **4.1. Kinetics constants at 20 °C**

219 **4.1.1. Desorption rate constant**

220 An example of kinetic experiments performed at 20 °C, in seawater devoid of phosphate is given in Fig. 2A.
221 Desorption of phosphate from sediment was relatively rapid until approaching an apparent equilibrium after about
222 25 hours.

223 Data were treated according to the logarithmic equation (15) described in section 2.2 which is illustrated in
 224 Fig. 2B. The phosphate concentration released at equilibrium (q_{Re}) was determined according to section 3.2.2 (all
 225 fits had $R^2 > 0.93$). The last time points were omitted for the computation due to the high uncertainties caused by
 226 the released phosphate approaching q_{Re} . The results are summarized in table 2.

227 An experiment (sediment S16; table 2) shows that desorption rate constants were very similar regardless of
 228 the solid-liquid ratio used. This narrow range of k_d ($0.0654 \pm 0.004 \text{ h}^{-1}$) at experimental sediment concentrations
 229 varying by a factor of 10 confirms that k_d is actually a constant. Overall desorption rates ranged between 0.057 h^{-1}
 230 and 0.128 h^{-1} with a mean value of $0.085 \pm 0.023 \text{ h}^{-1}$ (RSD: 27%).

231
 232 **Table 2** Results of desorption rate constant (k_d) determination obtained from the kinetic experiments
 233 according to the function described in Section 2.2.2

Station	S g L ⁻¹	n total	n*	R ²	Slope	q_i μmol g ⁻¹	q_{Re} μmol g ⁻¹	k_d h ⁻¹
S16	0.25	7	5	0.976	0.075	2.58	2.20	0.064
S16	0.5	7	5	0.980	0.102	2.58	1.72	0.068
S16	1	7	5	0.975	0.100	2.58	1.55	0.060
S16	2	7	5	0.978	0.126	2.58	1.41	0.069
S3	0.45	7	5	0.976	0.138	1.16	0.97	0.115
S10	0.5	7	4	0.994	0.125	0.74	0.57	0.097
S17	0.2	8	6	0.998	0.140	1.38	1.26	0.128
L23	0.25	7	5	0.983	0.100	5.39	2.99	0.056
G11b	0.5	11	9	0.972	0.090	2.01	1.29	0.058
RA	0.6	12	10	0.901	0.094	3.28	2.70	0.077
B1	0.5	11	7	0.901	0.117	1.64	1.34	0.096
AB	0.6	11	9	0.977	0.106	2.11	1.79	0.088
G7	0.5	8	6	0.870	0.101	1.10	1.00	0.092
B2	0.5	8	5	0.956	0.078	1.30	1.11	0.066

234 *Total n is the number of points of the kinetic experiments used to obtain q_{Re} by the asymptotic function. n^* is the number of data retained in the application of
 235 the logarithmic function for which R^2 and slope are given.

236 4.1.2. Adsorption rate constants (k_a and $k_a Q^\circ$)

237 Classically, k_a is the adsorption rate constant of the Langmuir theory which is deduced from the Langmuir
 238 coefficient b ($= k_a/k_d$) and the desorption rate constant k_d previously computed. The coefficient b is determined
 239 together with Q° by the Langmuir equations, using the IDE experiment data. However previous studies identified
 240 high standard errors for Q° , and for its associated coefficient b , when using these equations (Andrieux-Loyer and
 241 Aminot, 2023). A series of b and k_a computed in this way (table 3) illustrate the unrealistically wide range of k_a ,
 242 spanning 2 orders of magnitude. To overcome the problem of uncertainty of both b and Q° , required to obtain the
 243 adsorption rates, it is suggested to calculate these rates using the combined constant $k_a Q^\circ$. Indeed, that combined

244 constant is equal to $k_d K_p$, knowing that K_p is easily obtained from the IDE experiment data with an acceptable
 245 precision (Andrieux-Loyer and Aminot, 2023). Results are shown in Table 3. The range of the combined constant
 246 is rather narrow, 0.013 to 0.054 L g⁻¹, with a mean value of 0.028 L g⁻¹ (s: 0.011; RSD: ± 38%).

247

248

Table 3 Results of adsorption rate constants (k_a and $k_a Q^{\circ}$) determinations.

Station	k_d h ⁻¹	b L μmol ⁻¹	$k_a = bk_d$ L μmol ⁻¹ h ⁻¹	K_p L g ⁻¹	$k_a Q^{\circ} = k_d K_p$ L g ⁻¹ h ⁻¹
S16 (mean)	0.065	0.37	0.024	0.20	0.013
S3	0.115	0.93	0.108	0.21	0.024
S10	0.097	0.73	0.071	0.25	0.024
S17	0.128	0.62	0.079	0.42	0.054
L23	0.056	0.016	0.0009	0.31	0.017
G11b	0.058	0.79	0.046	0.64	0.037
RA	0.077	0.050	0.004	0.31	0.024
B1	0.096	0.36	0.034	0.35	0.033
AB	0.088	0.36	0.032	0.34	0.030
G7	0.092	-	-	0.26	0.024
B2	0.066	0.28	0.019	0.49	0.033

249

4.1.3 Salinity effect on rate constants

250

251

252

253

254

255

256

257

258

Although eutrophication occurs only in low turbid outer estuaries, in coastal waters of high salinity, an experiment was performed with a sediment similar to L23 to compare desorption constants k_d in two extreme conditions, sea water and pure demineralized water. The measured k_d of 0.071 and 0.105 h⁻¹, respectively, remain within the range of constants obtained for all the sediments tested in this study (section 4.1.1), which shows that the effect of salinity on desorption rates over the whole salinity range is not significant. In coastal waters this effect will be negligible. Regarding the adsorption constant $k_a Q^{\circ}$, which is a function of the partition coefficient K_p ($k_a Q^{\circ} = k_d K_p$; section 2.2), a slight effect may be expected which will depend on the nature of the fresh water used (dissolved ions and pH). However, within the range of values obtained in the various sediments tested (see Table 5) this effect is likely insignificant in the coastal areas subject to eutrophication events.

259

4.2. Temperature effect on rate constants

260

4.2.1. Comparison of released concentration

261

262

263

Phosphate release from the sediment at various temperatures is provided in Figure 3. Before further computation of rate constants, the effect of temperature on the amount of phosphate released at equilibrium has been examined.

264 Table 4 shows that final equilibrium concentrations lie between 2.13 and 2.20 $\mu\text{mol g}^{-1}$ within the
 265 temperature range while the computed q_{Re} lies between 2.06 and 2.22 $\mu\text{mol g}^{-1}$. Within the determined uncertainty
 266 of about ± 2 -4 percent, the equilibrium values are not significantly different at the 95% confidence level. Such
 267 variability appears consistent in experiments requiring multiple weighing of heterogeneous material such as
 268 sediments. Consequently, the equilibrium concentration can be assumed to be independent of temperature in the
 269 range 1-30 $^{\circ}\text{C}$ for most purposes.

270

271 **Table 4.** Final and computed equilibrium concentrations at the various temperatures.

Temperature	1 $^{\circ}\text{C}$	10 $^{\circ}\text{C}$	20 $^{\circ}\text{C}$	30 $^{\circ}\text{C}$
Maximum experiment time	400 h	200 h	50 h	30 h
Final PO_4 measured value $\mu\text{mol g}^{-1}$	2.15	2.13	2.19	2.20
Computed equilibrium PO_4 (q_{Re}) $\mu\text{mol g}^{-1}$	2.06	2.10	2.22	2.15
<i>standard error</i>	<i>0.05</i>	<i>0.05</i>	<i>0.09</i>	<i>0.05</i>

272

273 The partition coefficient K_p is required for the determination of the adsorption rate constant. It is computed
 274 as $K_p = q_e/C_e$ (see Table 1), with $q_e = q_i - q_{Re}$ and $C_e = q_{Re} \times S$. Since every term is constant K_p is independent of
 275 temperature in the 1-30 $^{\circ}\text{C}$ range. This result indicates that all K_p determined at 20 $^{\circ}\text{C}$ (Andrieux-Loyer and
 276 Aminot, 2023) are valid regardless of the temperature encountered in most coastal environments. In the present
 277 experiments, the reference value of q_{Re} was taken as the average of the equilibrium values at 20 and 30 $^{\circ}\text{C}$
 278 (2.18 $\mu\text{mol g}^{-1}$), to avoid a risk that slightly lower values at 1 and 10 $^{\circ}\text{C}$ might result from potentially too short
 279 experimental durations. Hence, with $q_i = 2.46 \mu\text{mol g}^{-1}$, $q_{Re} = 2.18 \mu\text{mol g}^{-1}$ and $S = 0.25 \text{ g L}^{-1}$, one obtained $K_p =$
 280 0.514 L g^{-1} .

281 The so-called Langmuir coefficient b ($b = k_a/k_d$) is linked to K_p by the relation $K_p = b(Q^{\circ} - q_e)$. Since K_p , Q°
 282 (maximum adsorption capacity) and q_e are constant, b is also constant in the temperature range 1-30 $^{\circ}\text{C}$.
 283 Consequently, the two rate constants k_a and k_d show similar variations in relation to temperature so that their ratio
 284 is independent of temperature.

285

286 **4.2.2 Determination of temperature effect on rate constants**

287 The logarithmic function, which enables the computation of k_d , includes the difference between q_{Re} and
 288 PO_4 released at any times. The q_{Re} value of 2.18 $\mu\text{mol g}^{-1}$ previously used for the determination of K_p , was also
 289 used in the computation of k_d (section 4.2.2). Since q_{Re} exhibits an uncertainty of a few percents, experimental data

290 too close to q_{Re} were omitted to improve the precision. Consequently, only the 5-6 measures of PO_4 released up to
 291 20 hours were considered for computation. The results are illustrated in Fig. 4A and summarized in table 5.

292

293 **Table 5** Results of rate constants (k_d , k_a and k_aQ°) obtained at various temperatures. Common main data:

294 $S = 0.25 \text{ g L}^{-1}$; q_i (= exch-P) = $2.46 \text{ } \mu\text{mol g}^{-1}$; $q_{Re} = 2.18 \text{ } \mu\text{mol g}^{-1}$; $K_p = 0.514 \text{ L g}^{-1}$.

Temperature °C	ln function		k_d h ⁻¹	$k_aQ^\circ = k_dK_p$ L g ⁻¹ h ⁻¹
	R ²	Slope		
1	0.982	0.0339	0.0300	0.0154
10	0.983	0.0521	0.0462	0.0237
20	0.963	0.0799	0.0708	0.0364
30	0.988	0.1360	0.1205	0.0619

295

296

297 Variation of k_d as a function of temperature is exponential (Fig. 4B) according to $k_d = 0.0285e^{0.0473 \times t}$. The
 298 adsorption constant k_aQ° is obtained as: $k_dK_p = k_a \times 0.514$. Schematically the kinetics constants increase by a factor
 299 of about 1.6 for every 10 Celsius degree increase.

300

301 **4.2.3. Activation energy and adsorption process**

302

303 According to the Arrhenius law, k_d can be expressed as:

$$304 \quad k_d = A e^{-\frac{E_a}{RT}}$$

305 with A = Arrhenius factor, E_a = activation energy (J mol⁻¹), R = universal gas constant (8.314 J mol⁻¹ K⁻¹) and T =
 306 absolute temperature (K).

307 The activation energy for phosphate sorption in our experiments was obtained by plotting $\ln(k_d) =$
 308 $\ln(A) - E_a/RT$ vs $1/T$ (Fig. 5). The value found for E_a (product of the slope by R , after sign changed), was: $E_a =$
 309 $32.65 \text{ kJ mol}^{-1}$.

310

311

312

313 5. DISCUSSION

314 5.1. Kinetics constants at 20°C

315 Desorption of phosphate from sediment approaching an apparent equilibrium after about 25 hours is in
316 agreement with previously published results on phosphate desorption from soils (Vaidyanathan and Talibudeen,
317 1970). Unfortunately, despite a wide literature search, no desorption rate constant value could be found for
318 sediments into water. Shariatmadari et al. (2006) used the first order model to describe P release from Iranian
319 calcareous soils amended with a phosphate solution (about 1 $\mu\text{mol g}^{-1}$) for 1 month before desorption in CaCl_2
320 solutions. They report desorption rate constants from 0.0388 to 0.0611 h^{-1} , in the same range as our values
321 (0.057 h^{-1} to 0.128 h^{-1}), but the different methodologies may affect the results and bias the comparison.

322 Our data highlight that coastal sediments are able to release half their exchangeable phosphate in a few
323 hours in a water devoid of phosphate. Almost total consumption of phosphate is frequent in coastal water during
324 spring and summer after phytoplankton blooms. In these environments the high dynamic conditions due to tides
325 contribute to the resuspension of superficial bottom sediments which are a potential source of phosphate.
326 Overlooking this compartment would be a major gap in ecological models of coastal waters (Baretta et al,1995)
327 mainly with the increasing storm frequency (Garnier et al., 2018), intensity and duration (Stockwell et al., 2019)
328 which could increase resuspensions events ((Tammeorg et al., 2013).

329 Most studies dealing with phosphorus in sediments focus on the amount of phosphorus liable to be retained
330 on the sediment as a phosphate reservoir, but not on the kinetics of the process. The rare adsorption rate constants
331 we found were obtained in experimental conditions very different of ours. In a study by Tang et al. (2014),
332 sediments of a drinking water reservoir in China were loaded with phosphate solutions, but at sediment and
333 phosphorus concentrations up to one hundred times greater than ours. Additionally, our experiments show that a
334 reliable adsorption rate constant k_a cannot be obtained from the Langmuir equation. Although this problem can be
335 overcome by using the operational combined constant $k_a Q^\circ$. the latter cannot be compared with other literature
336 values.

337 In our study, we selected sediments with differing grain sizes since the nature of particles may affect surface
338 interactions with phosphate and modify the exchange rates with surrounding water. The relationship between the
339 rate constants and the proportion of fine particles ($< 63 \mu\text{m}$) was thus examined (Fig.6).

340 For k_d , lower constants are generally associated with higher concentrations of fine particles (Fig. 6A). The
341 slope of the linear regression ($R^2 = 0.40$) is significant at the 95 % confidence level with a p-value of 0.036.

342 However, the variation over the whole range of proportion of fine particles remains narrow with a mean (\pm s) of
343 $0.085 \pm 0.023 \text{ h}^{-1}$. The combined adsorption constant $k_a Q^{\circ}$ appears independent of the sediment grain size (Fig. 6B),
344 with a p-value of 0.99 for the regression slope and a mean (\pm s) of $0.028 \pm 0.011 \text{ h}^{-1}$. Consequently, the mean
345 values could be an acceptable choice for models in a first approach.

346 The quasi-independence of rate constants with the proportion of fine particles suggests that these particles
347 exhibit the main interaction with phosphate whatever the amount of the coarse fraction of the sediment.

348

349 **5.2. Temperature effect on rate constants**

350 Estuarine and coastal waters are subjected to marked water temperature oscillations in diurnal and seasonal
351 cycles. For example, in the Bay of Seine, our studies show that temperature varies from 5-6 °C in winter to 16-17
352 °C in summer. Because of the high dynamics induced by the tide, the water is almost homogeneous from surface
353 to bottom, with no thermocline at any time. Bottom sediments resuspended in the water column are therefore
354 submitted to higher temperatures in summer when water phosphate concentrations are depleted following
355 phytoplankton growth.

356 Our experiments show an increase of the rate constants by a factor of 4 between 1 °C and 30 °C while the
357 final phosphate concentration released from the sediment remains independent of temperature within a coefficient
358 of variation of a few percents. A noticeable result is that the two rate constants k_a and k_d show similar variations
359 in relation to temperature. Using the law of temperature dependence of the rates, deduced from the experiments,
360 modeling phosphate dynamic exchanges between sediment and seawater becomes possible. This is a step forward
361 beyond the concept of the sediment as a phosphate reservoir.

362 An additional result is that K_p determined at 20 °C is valid regardless of the temperature (range 1-30 °C).
363 This simplifies the laboratory procedure if the ability of a sediment to exchange with surrounding water at any
364 temperature should be inferred from sediment exchangeable phosphate and water phosphate concentration
365 (Andrieux-Loyer and Aminot, 2023). Indeed, this allows a single IDE experiment to be performed at room
366 temperature.

367 In this study, the determination of the magnitude of activation energy (E_a) can provide insight into the type
368 of molecular bounds encountered (physical or chemical). According to Saha et al (2010) the activation energy for
369 physisorption is usually no more than 40 kJ mol⁻¹ since the forces involved in physisorption are weak. In their

370 study, Inglezakisa and Zorpas (2012) found that most of their E_a values for physisorption are below the higher
371 limit of 40 kJ mol⁻¹ found in literature, while the 24-40 kJ mol⁻¹ range corresponds to ionic exchanges.

372 The value found for E_a was: $E_a = 32.65$ kJ mol⁻¹. This agrees with the above range for physisorption, mainly
373 governed by ionic mechanisms (Inglezakisa and Zorpas, 2012). For lake sediments, Topçu et al. (2018) found E_a
374 in the range 3-11 kJ mol⁻¹ while the value of 48.5 kJ mol⁻¹ was reported by Omari et al. (2019) using sediments of
375 a Morocco wadi (riverbed). The differences may be attributed to the sediment types but all values remain lower or
376 close to the 40 kJ mol⁻¹ criterion below which physisorption is the dominant process.

377 6. CONCLUSION

378 This work aimed to determine the kinetic behavior for the adsorption-desorption processes of phosphate on
379 coastal sediments. Relying on the Langmuir theory, adapted to solid-water exchanges in natural environments, it
380 was possible to determine the rate constants for adsorption and desorption processes. The desorption constant is
381 little influenced by sediment grain size with a RSD of only 27% over the whole range of fine fraction (0-100% <
382 63 µm) and the combined adsorption constant is independent of grain size. The variation of the rate constants in
383 relation to temperature was established in the range 1-30 °C showing that the rates increase approximately by a
384 1.6 factor for a 10 °C increase. Ionic physisorption of phosphate on coastal sediments agrees with our activation
385 energy results. The partition coefficient and the Langmuir constant (rate constants ratio) were independent of
386 temperature over the tested range. These results are essential to develop environmental models which need to
387 include the sediment phase as a contributor to phosphate cycling in estuarine and coastal systems.

388

389 **Acknowledgements** We thank Roger K rouel, Xavier Philippon, Agn s Youenou, Anne Daniel-Scuiller,
390 Marie-Madeleine Danielou and Erwan Le Gall for their collaboration during the sampling surveys in the Bay of
391 Seine and the Penz  estuary and our colleagues working for the national monitoring network (R seau National
392 d'Observation) for their help during the cruises in the Loire and Gironde estuaries. Roger K rouel, brought
393 assistance for laboratory work. We are grateful to Yann Aminot for his constructive comments and for language
394 review.

395 **Author contributions** The two authors have participated in the research and article preparation (Study's
396 conception, acquisition of samples, phosphate analysis, writing of the manuscript).

397 **Funding** This work was partially funded by the research program PNOC (Programme National d'Océanographie
398 Côtière) and by the project ICREW (Improving Coastal and Recreational Waters).

399 **Data availability** The data presented in the current study are available from the corresponding author upon
400 request.

401 **Conflict of interest** The authors declare that they have no conflicts of interest.

402

403 **References**

404 Ait Ballagh FE, Rabouille C, Andrieux-Loyer F, Soetaert K, Elkalay K, Khalil K (2020) Spatio-temporal
405 dynamics of sedimentary phosphorus along two temperate eutrophic estuaries: A data-modelling approach.
406 Continental Shelf Research 193: 1-23.

407 Ait Ballagh FE, Rabouille C, Andrieux-Loyer F, Soetaert K, Lansard B, Bombléd B, Monvoisin G, Elkalay
408 K, Khalil K (2021) Spatial Variability of Organic Matter and Phosphorus Cycling in Rhône River Prodelta
409 Sediments (NW Mediterranean Sea, France): a Model-Data Approach. Estuaries and Coasts 44(7): 1765-1789.

410 Aminot A, Andrieux F (1996) Concept and determination of exchangeable phosphate in aquatic sediments.
411 Water Research 30: 2805-2811.

412 Aminot A, Kérouel R, Coverly SC (2009) Nutrients in seawater using segmented flow analysis. In: Wurl
413 O (ed) Practical guidelines for the analysis of seawater. CRC Press, Boca Raton, pp 143–178.

414 Andrieux-Loyer, Aminot (2023) Assessing exchangeable phosphate and related data in coastal sediments:
415 Theoretical and practical considerations. Estuarine, Coastal and Shelf Science 281: 108218.

416 Andrieux-Loyer F, Azandegbe A, Caradec F, Philippon X, Kerouel R, Youenou A, Nicolas JL (2014)
417 Impact of oyster farming on Diagenetic Processes and the Phosphorus Cycle in Two Estuaries (Brittany, France).
418 Aquatic Geochemistry 20(6): 573-611

419 Baretta JW, Ebenhöf W, Ruardij P (1995) The European regional seas ecosystem model, A complex marine
420 ecosystem model. Netherlands Journal of Sea Research 33(3/4): 233-246.

421 Boesch DF (2002) Challenges and opportunities for science in reducing nutrient over-enrichment of coastal
422 ecosystems. Estuaries 25:744-758.

- 423 Cha HJ, Lee CB, Kim BS, Choi MS, Ruttenger KC (2005) Early diagenetic redistribution and burial of
424 phosphorus in the sediments of the southwestern East Sea (Japan Sea). *Marine Geology* 216: 127-143.
- 425 Couceiro F, Fones GR, Thompson CEL, Statham PJ, Sivyer DB, Parker R, Kelly-Gerrey BA, Amos CL
426 (2013) Impact of resuspension of cohesive sediments at the Oyster Grounds (North Sea) on nutrient exchange across
427 the sediment-water interface. *Biogeochemistry* 113: 37-52.
- 428 Garnier E, Ciavola P, Spencer T, Ferreira O, Armaroli C, McIvor A (2018) Historical analysis of storms
429 events: Cases studies in France, England, Portugal and Italy. *Coastal Engineering* 134: 10-23.
- 430 Inglezakisa VJ, Zorpas AA (2012). Heat of adsorption, adsorption energy and activation energy in
431 adsorption and ion exchange systems in *Desalination and Water Treatment* 39:149–157.
- 432 Jarvies HP, Withers JA, Neal C (2002). Review of robust measurement of phosphorus in river water:
433 sampling, storage, fractionation and sensitivity. *Hydrology and Earth System Sciences Discussions*, European
434 Geosciences Union 6(1):113-131.
- 435 Li M, Whelean MJ, Wang GQ, White SM (2013) Phosphorus sorption and buffering mechanisms in
436 suspended sediments from the Yangtze Estuary and Hangzhou Bay, China. *Biogeosciences* 10:3341-3348.
- 437 Murphy J, Riley JR (1962) A modified single solution method for the determination of phosphate in natural
438 waters. *Analytica Chimica Acta* 27:31-36.
- 439 Omari H, Dehbi A, Lammini A, Abdallaoui A (2019) Study of the Phosphorus Adsorption on the
440 Sediments. *Journal of Chemistry* 2019: ID 2760204, 10 pages
- 441 Otero M, Coelho JP, Rodrigues ET, Pardal MA, Santos EBH, Esteves VI, Lille
442 bo AI (2013) Kinetics of the PO₄-P adsorption onto soils and sediments from the Mondego estuary
443 (Portugal). *Marine Pollution Bulletin* 77:361-366.
- 444 Saha P, Chowdhury S, Gupta S, Kumar I (2010) Insight into adsorption equilibrium, kinetics and
445 thermodynamics of Malachite Green onto clayey soil of Indian origin. *Chemical Engineering Journal* 165: 874-
446 882.
- 447 Seitzinger SP, Harrison JA, Dumont E, Beusen AHW, Bouwman A.F (2005) Sources and delivery of
448 carbon, nitrogen, and phosphorus to the coastal zone: An overview of Global Nutrient Export from Watersheds
449 (NEWS) models and their application. *Global Biological Cycles* 19(4): GB4S01.
- 450 Shariatmadari H, Shirvani M, Jafari A (2006) Phosphorus release kinetics and availability in calcareous
451 soils of selected arid and semiarid toposequences. *Geoderma* 132: 261-272.

- 452 Smil V (2000) Phosphorus in the environment: natural flows and human interferences. *Annual Review of*
453 *Energy Environment* 25:53–88.
- 454 Sondergaard, Kristensen P, Jeppesen E (1992) Phosphorus release from resuspended sediment in the
455 shallow and wind-exposed Lake Arreso, Denmark. *Hydrobiologia* 228: 91-99.
- 456 Stockwell JD, Doubek JP, Adrian R, Anneville O, Carey CC, Carvalho L, De Senerpont Domis LN, Dur
457 G, Frassl MA, Grossart H-P, Ibelings BW, Lajeunesse MJ, Lewandowska AM, Llamas ME, Matsuzaki SS, Nodine
458 ER, Nöges P, Patil VP, Pomati F, Rinke K, Rudstam LG, Rusak JA, Salmaso R, Seltmann CT, Straile D, Thackeray
459 SJ, Thiery W, Urrutia-Cordero P, Venail P, Verburg P, Woolway RI, Zohary T, Andersen MR, Bhattacharya R,
460 Hejzlar R, Janatian N, Kpodonu ATNK, Williamson TJ, Wilson HL (2019) Storm impacts on phytoplankton
461 community dynamics in lakes. *Global Change Biology* 26 (5): 2756-2784.
- 462 Tammeorg O, Niemistö J, Möls T, Laugaste R, Panksep K, Kangur K (2013) Wind-induced sediment
463 resuspension as a potential factor sustaining eutrophication in large and shallow Lake Peipsi. *Aquatic Science* 75:
464 559-570.
- 465 Tang X, Wu M, Dai X, Chai P (2014) Phosphorus dynamics and adsorption characteristics for sediment
466 from a drinking water source reservoir and its relation with sediment compositions. *Ecological Engineering*
467 64:276-284.
- 468 Topçu A, Ulusoy U, Pulatsü S (2018) Determination of sediment phosphate sorption characteristics in
469 shallow Mogan lake, Turkey. *Applied Ecology and Environmental Research* 16(5): 5971-5985.
- 470 Van Raaphorst W, Kloosterhuis HT (1994) Phosphate adsorption in superficial intertidal sediments. *Marine*
471 *Chemistry* 48:1-16.
- 472 Vaidyanathan LV, Talibudeen O (1970) Rate processes in the desorption of phosphate from soils by ion-
473 exchange resins. *Journal of Soil Science* 21(1): 173-183.
- 474 Wang X, Zhang L, Zhang H, Wu X, Mei D (2012) Phosphorus adsorption characteristics at the sediment–
475 water interface and relationship with sediment properties in FUSHI reservoir, China. *Environmental Earth*
476 *Sciences* 67: 15-22.
- 477 Wang S, Vogt RD, Carstensen J, Lin Y, Feng J, Lu X (2022) Riverine flux of dissolved phosphorus to the
478 coastal sea may be overestimated, especially in estuaries of gated rivers: Implications of phosphorus
479 adsorption/desorption on suspended sediments. *Chemosphere* 287: 132206.

480 Voice TC, Weber WJr (1983) Sorption of hydrophobic compounds by sediments, soils and suspended
481 solis-I. Theory and backgtound. Water Research 17(10): 1433-1441.

482 Zhang B, Fang F, Guo JS, Chen YP, Li Z, Guo SS (2012) Phosphorus fractions and phosphate sorption-
483 release characteristics relevant to the soil composition of water-level-fluctuating zone of Three Gorges Reservoir.
484 Ecological Engineering 40: 153-159.

485 Zhou A, Tang H, Wang D (2005) Phosphorus adsorption on natural sediments: Modeling and effects of pH
486 and sediment composition. Water Research 39: 1245-1254

487
488
489
490
491
492
493
494
495
496
497
498
499
500
501
502
503
504
505
506
507
508
509
510
511
512
513
514
515
516
517
518
519
520
521
522
523
524
525

Journal Pre-proof

526 **Figure captions**

527

528 **Fig. 1.** Comparison of kinetics performed on sediments freshly treated and treated after lyophilisation. Two
 529 sediments from the Bay of Seine with different exchangeable phosphate concentrations were used.

530 **Fig. 2.** A: Kinetics experiment performed with the sediment from station 17 of the Bay of Seine ($S = 0.2 \text{ g}$
 531 L^{-1}); B: Determination of the desorption rate constants (k_d) by plotting $\ln(q_{Re}/(q_{Re} - q_{Rt}))$ versus time;

532 $k_d = \text{slope} \times (q_{Re}/q_i)$

533 **Fig. 3.** Release of phosphate from the same sediment (Bay of Seine, station 16), at increasing temperatures
 534 (note the two time scales)

535 **Fig. 4.** A: logarithmic functions of kinetics of phosphate release as a function of time. B: variation of the
 536 adsorption constant k_d as a function of temperature.

538 **Fig. 5.** Plot of $\ln(k_d)$ versus $1/T$ for estimation of activation energy (E_a ; kJ mol^{-1})

539

540 **Fig. 6.** A: Distribution of the desorption constant k_d and B: the combined adsorption constant $k_a Q^0 (= k_d K_p)$
 541 as a function of the $< 63 \mu\text{m}$ sediment fraction, in selected sediments covering this fine fraction range.

542

543

544
545
546
547
548
549
550
551
552
553
554
555
556
557
558
559
560
561
562
563
564
565

Table captions

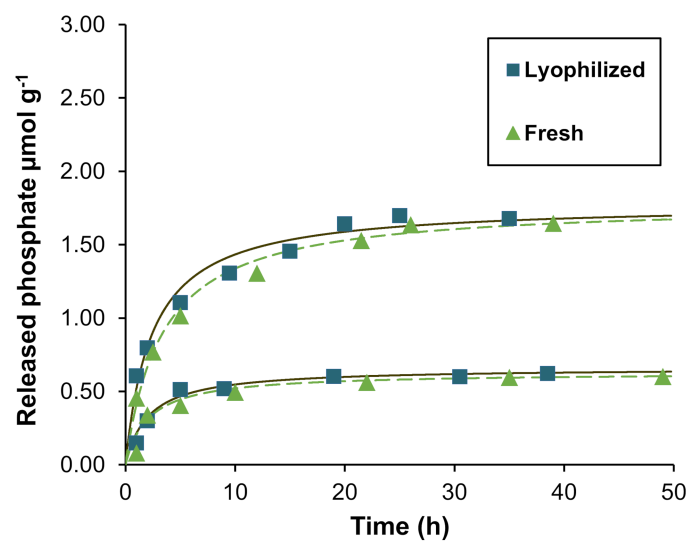
Table 1 Nomenclature used herein

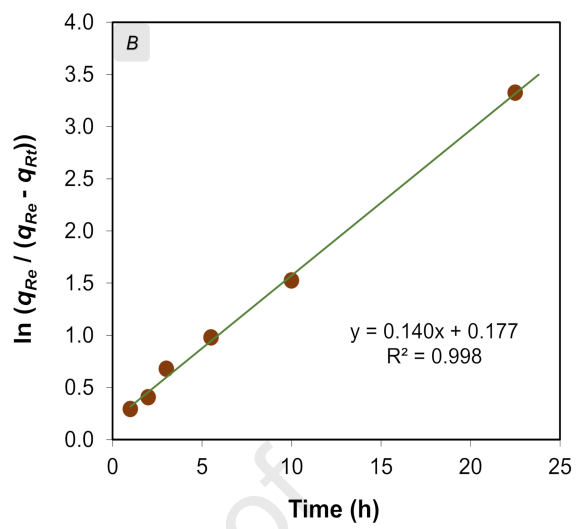
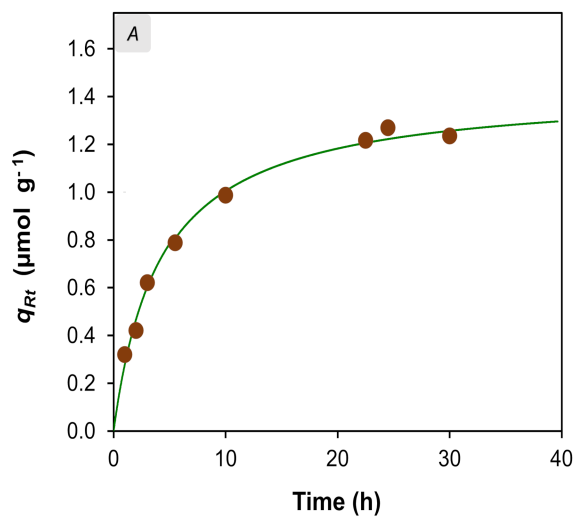
Table 2 Results of desorption rate constant (k_d) determination obtained from the kinetic experiments according to the function described in Section 2.2.2

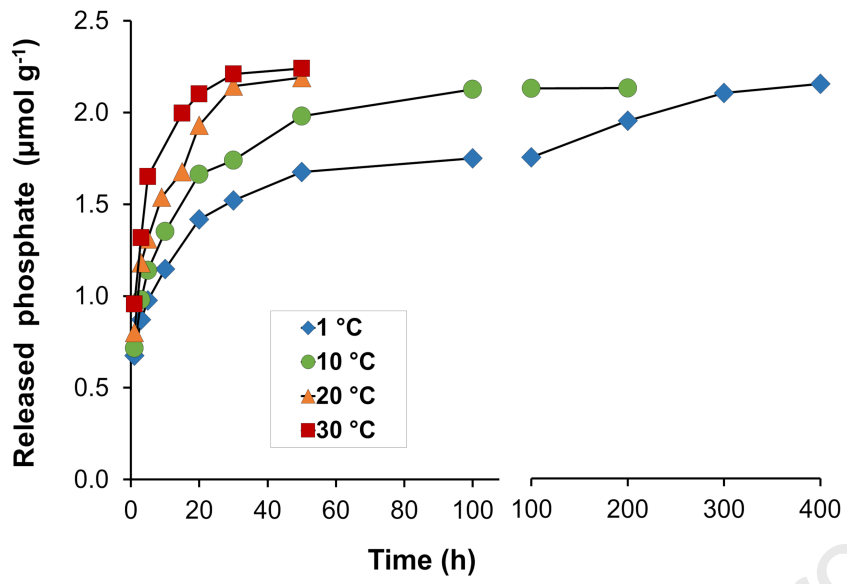
Table 3 Results of adsorption rate constants (k_a and $k_a Q^\circ$) determinations

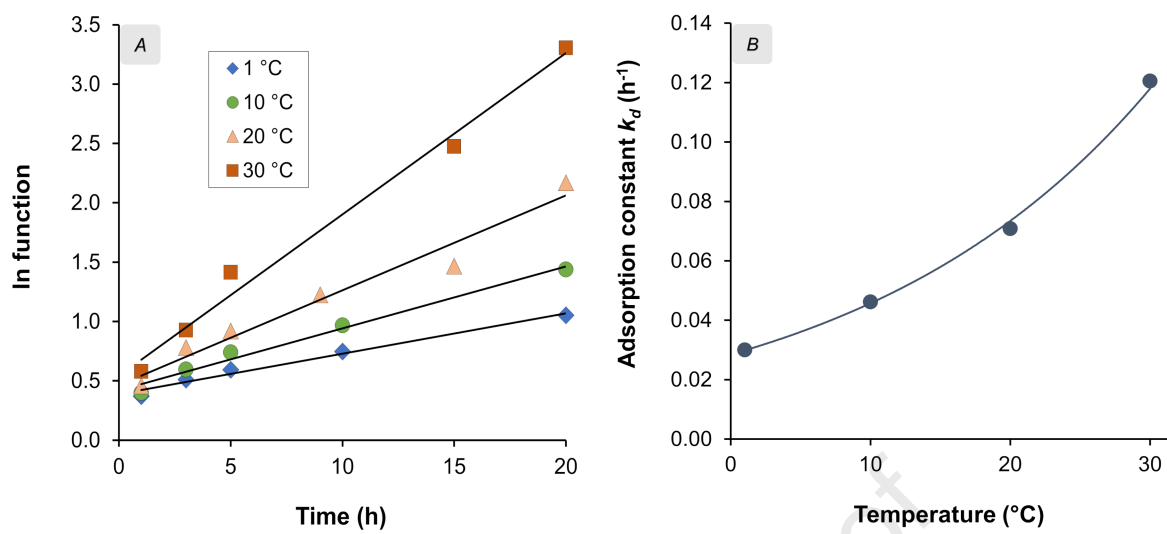
Table 4 Final and computed equilibrium concentrations at the various temperatures

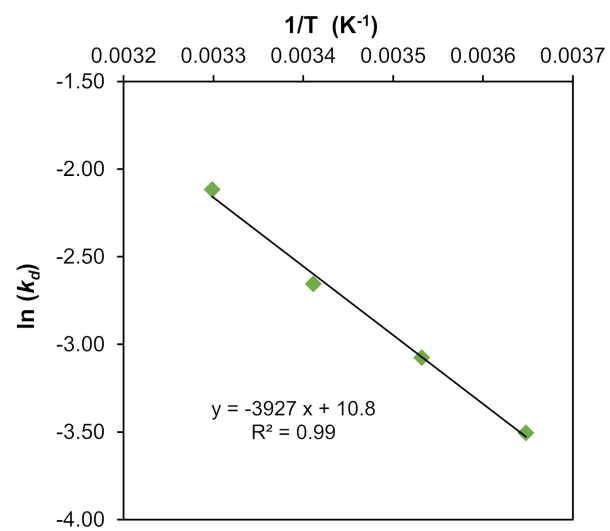
Table 5 Results of rate constants (k_d , k_a and $k_a Q^\circ$) obtained at various temperatures. Common main data:
 $S = 0.25 \text{ g L}^{-1}$; q_i (= exch-P) = $2.46 \text{ } \mu\text{mol g}^{-1}$; $q_{Re} = 2.18 \text{ } \mu\text{mol g}^{-1}$; $K_p = 0.514 \text{ L g}^{-1}$



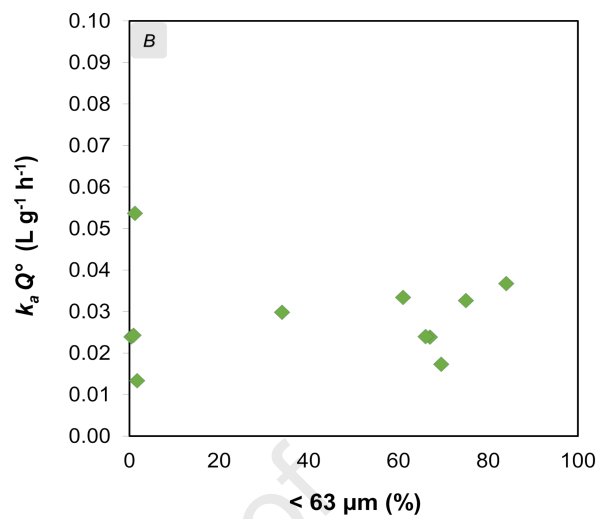
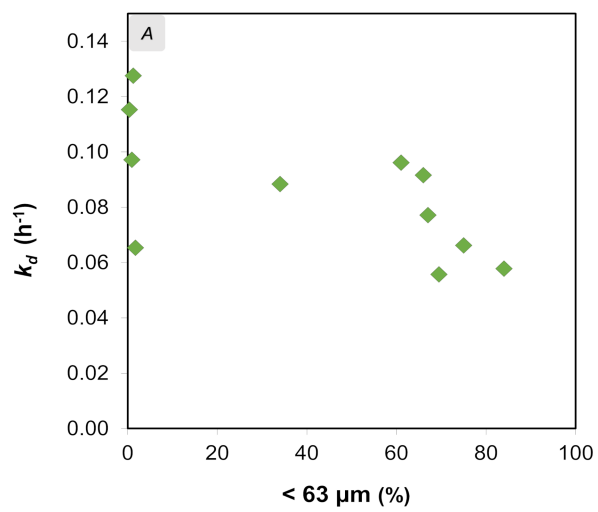








Journal Pre-proof



Highlights

- Kinetics of Langmuir-treated phosphate exchange between coastal sediments and water
- Determination of rate constants with highlight on a combined adsorption constant
- Adsorption and desorption rate constants: little dependent on sediment grain size
- The temperature factor of rate constants is 1.6 for each 10 °C in the range 1-30 °C

Journal Pre-proof

Declaration of interests

The authors declare that they have no known competing financial interests or personal relationships that could have appeared to influence the work reported in this paper.

The authors declare the following financial interests/personal relationships which may be considered as potential competing interests:

Journal Pre-proof